



MRS. ISRAA ABDALLA MOUSTAFA SLIEM (Orcid ID : 0000-0001-9708-4017)

DR SIVA S PANDA (Orcid ID : 0000-0003-3668-104X)

DR RIHAM GEORGE (Orcid ID : 0000-0002-2493-1315)

DR RAJEEV SAKHUJA (Orcid ID : 0000-0002-9284-9137)

Article type : Research Article

Design, synthesis, antimicrobial and DNA gyrase inhibitory properties of fluoroquinolone-dichloroacetic acid hybrids

Israa A. Seliem ^{a,b}, Siva S. Panda ^{a,*}, Adel S. Girgis ^c, Yosra I. Nagy ^d, Riham F. George ^e, Walid Fayad ^f, Nehmedo G Fawzy ^c, Tarek S. Ibrahim ^{b,g}, Amany M. M. Al-Mahmoudy ^b, Rajeev Sakhuja ^h, Zakaria K. M. Abdel-samii ^b

^a *Department of Chemistry & Physics, Augusta University, Augusta, GA 30912, USA.*

^b *Department of Pharmaceutical Organic Chemistry, Faculty of Pharmacy, Zagazig University, Zagazig, 44519, Egypt.*

^c *Department of Pesticide Chemistry, National Research Centre, Dokki, Giza 12622, Egypt.*

^d *Microbiology and Immunology Department, Faculty of Pharmacy, Cairo University, Cairo 11562, Egypt.*

^e *Pharmaceutical Chemistry Department, Faculty of Pharmacy, Cairo University, Cairo 11562, Egypt.*

^f *Drug Bioassay-Cell Culture Laboratory, Pharmacognosy Department, National Research Centre, Dokki, Giza, 12622. Egypt.*

This article has been accepted for publication and undergone full peer review but has not been through the copyediting, typesetting, pagination and proofreading process, which may lead to differences between this version and the [Version of Record](#). Please cite this article as [doi: 10.1111/CBDD.13638](https://doi.org/10.1111/CBDD.13638)

This article is protected by copyright. All rights reserved

^g Department of Pharmaceutical Chemistry, Faculty of Pharmacy, King Abdulaziz University, Jeddah, 21589, Saudi Arabia.

^h Department of Chemistry, Birla Institute of Technology and Science, Pilani 333031, Rajasthan, India.

* Corresponding author. E-mail: sspanda12@gmail.com, sipanda@augusta.edu

Tel: +1-706-667-4022; fax: +1-706-667-4519

Running head: fluoroquinolone-dichloroacetic acid hybrid conjugates

Keywords: Fluoroquinolone, Dichloroacetic acid, Antibacterial, Hybrid conjugates, DNA gyrase.

Abstract

A series of new fluoroquinolone conjugates **8a–g** and **9a–f** were synthesized via benzotriazole-mediated synthetic approach with good yield and purity. Some of the synthesized analogs exhibited significant antibacterial properties against *E. coli* and *S. aureus* with potency higher than that of the parent drugs through in vitro standard bio-assay procedure (conjugates **8c** and **8d** reveal antimicrobial properties with potency 1.9, 61.9, 20.7 and 2.4, 37.1, 8.3 folds relative to the parent antibiotic **6** against *E. coli*, *S. aureus* and *E. faecalis*, respectively). The observed experimental data supported by enzymatic DNA gyrase inhibitory property. Developed BMLR-QSAR model validates the observed experimental data and recognizes the parameters responsible for the enhanced antibacterial properties.

Introduction

Bacterial infections caused by both Gram-positive and Gram-negative pathogens are responsible for the majority of hospital-acquired infections, which affects the global healthcare systems (Peleg & Hooper, 2010). According to the latest World Health Organization (WHO) report, around 10 million deaths every year (over 15% of all deaths) are due to infectious disease (Balaban et al., 2016). In addition, the drug resistance organisms keep on increasing at an alarming

rate associated with considerable mortality (Sprenger & Fukuda, 2016). This forces an immense need to develop potential antimicrobial agents active against both drug sensitive and drug-resistant bacterial infections (Brown & Wright, 2016; Silver, 2011).

Quinolone and fluoroquinolones are among different class of antibiotics used for the treatment of bacterial infections (Fig. 1). The pharmacological importance of fluoroquinolones is continually attracting medicinal chemists' to use as a scaffold for the development of potent antibacterial agents. Fluoroquinolones can show adverse effects in the central nervous system, skin and gastrointestinal tract (Sarro & Sarro, 2001). Over the past few years, different positions of the fluoroquinolones were modified to improve the potency and overcome the associated drug resistance (Towle et al., 2018; Bartzatt et al., 2013; Allaka et al., 2016; Zhang et al., 2014; Rajulu et al., 2014).

Dichloroacetate (DCA) is known for inhibition of pyruvate dehydrogenase kinase (PDK), which is a key step that leads to reestablishment of the mitochondrial oxidative phosphorylation pathway (Sutendra & Michelakis, 2013). Although, the preliminary study of DCA shows the slowdown growth of certain tumors the mechanism is not well developed. Several antitumor agents show improved efficacy when taken in combination with DCA (Florio et al., 2018). As far as we are aware, only one article reported the dichloroacetic acid derivatives for antibacterial properties (Casini et al., 1966).

Insert fig. 1

The present study describes synthesis of quinolone conjugates with amino acids to improve the antibacterial property and increase the cell-permeability (Faidallah et al., 2018; Panda et al., 2016; Panda et al., 2015; Tiwari et al., 2014; Panda et al., 2014; Ibrahim et al., 2014). The present work focuses on ciprofloxacin and norfloxacin, second-generation fluoroquinolone that inhibits DNA gyrase and topoisomerase IV. For the first time herein, we report the hybrid conjugates of DCA and fluoroquinolone, which may overcome the resistance while maintaining or improving the antibacterial property as well as diminishing associated adverse effects.

E. coli, *P. aeruginosa*, *S. aureus* and *E. faecalis* were selected for the synthesized hybrid conjugate screening because of their physiological relevance and close relation to pathogenic strains which cause several diseases in humans.

Experimental Section

Chemistry

Melting points were determined on a capillary point apparatus equipped with a digital thermometer. NMR spectra were recorded in (DMSO- d_6) on Bruker NMR spectrometers operating at 500 MHz for ^1H (with TMS as an internal standard) and 125 MHz for ^{13}C . All microwave assisted reactions were carried out with a single mode cavity Discover Microwave Synthesizer (CEM Corporation, NC). The reaction mixtures were transferred into a 10 mL glass pressure microwave tube equipped with a magnetic stirrer bar. The tube was closed with a silicon septum and the reaction mixture was subjected to microwave irradiation (Discover mode; run time: 60 s; Power Max-cooling mode).

General procedure for the preparation of *N*-(Boc-aminoacyl)-benzotriazoles 10a–g (Panda et al., 2014).

Compounds **10a–g** were synthesized by irradiating an equimolar amount of Boc protected amino acid with 1-(methylsulfonyl)-1H-benzo[d][1,2,3]triazole (BtSO₂Me) in the presence of 2.0 eq. of triethylamine for 2 min run time and 60 min hold time at 70 °C and 50 W irradiation power. Completion of the reaction was monitored by TLC. After completion of the reaction, the mixture was quenched with water. The product obtained extracted with ethyl acetate and then washed with a saturated solution of sodium carbonate and water to afford compound **10a–g**.

General procedure for the synthesis of Boc-protected amino acid-fluoroquinolone conjugates 11a–g and 12a–f

A dried heavy-walled Pyrex tube containing a small stir bar was charged with *N*-(Boc-aminoacyl)benzotriazoles (1.0 eq.) and fluoroquinolone (1.0 eq.) dissolved in DMF along with triethylamine (2.0 eq.). The reaction mixture was exposed to microwave irradiation (20 W) at 50 °C for 60 min. Each mixture was allowed to cool through an inbuilt system until the temperature fell below 30 °C (ca. 10 min). Each reaction mixture was quenched with ice cold water and the solid obtained was filtered and washed with 4N HCl and water to give the desired compound.

General procedure for the synthesis of hybrid conjugates 8a-g and 9a-f

Boc protected amino acid-fluoroquinolone conjugate was stirred in HCl gas saturated dioxane for 2 h. Dioxane was evaporated under reduced pressure and the residue was treated with diethyl ether. The resultant solid was treated without further purification with benzotriazole

derivatives of DCA **3** in the presence of triethylamine (2.0 eq.) in acetonitrile-water mixture (3.5 mL + 1.5 mL) and stirred at room temperature for 4-6 h. Acetonitrile was removed under vacuum and the residue quenched in ice cold water. The precipitate obtained was washed with 4N HCl, water and then dried over vacuum to obtain the desired hybrid conjugates **8a-g** and **9a-f**.

*(S)*1-cyclopropyl-7-(4-((2,2-dichloroacetyl)glycyl)piperazin-1-yl)-6-fluoro-4-oxo-1,4-dihydroquinoline-3-carboxylic acid (DCA-L-Gly-Cip, **8a**).

White microcrystals, m.p 241–243 °C, yield 61%. IR: $\nu_{\max}/\text{cm}^{-1}$ 3300, 3010, 2923, 1702, 1247, 1114, 804; ^1H NMR (DMSO- d_6) δ : 15.17 (s, 1H), 8.72–8.67 (m, 2H), 7.92 (d, $J = 12.4$ Hz, 1H), 7.58 (s, 1H), 6.70 (s, 1H), 4.20–4.14 (m, 2H), 4.10–4.06 (m, 1H), 3.89–3.54 (m, 8H), 1.35–1.30 (m, 2H), 1.22–1.17 (m, 2H). ^{13}C NMR (DMSO- d_6) δ : 176.3, 166.1, 165.9, 163.7, 152.0, 148.0, 144.8, 139.2, 118.9, 111.1, 111.0, 106.7, 66.5, 49.3, 49.1, 43.7, 42.3, 41.2, 35.9, 7.6. HRMS m/z for $\text{C}_{21}\text{H}_{21}\text{Cl}_2\text{FN}_4\text{O}_5$ $[\text{M}+\text{Na}]^+$ Calcd. 521.0765. Found: 521.077

*(S)*1-cyclopropyl-7-(4-((2,2-dichloroacetyl)-L-alanyl)piperazin-1-yl)-6-fluoro-4-oxo-1,4-dihydroquinoline-3-carboxylic acid (DCA-L-Ala-Cip, **8b**).

White microcrystals, m.p 253–255 °C, yield 73%. IR: $\nu_{\max}/\text{cm}^{-1}$ 3371, 3010, 2865, 1696, 1245, 1113, 805; ^1H NMR (DMSO- d_6) δ : 13.84 (br s, 1H), 8.92 (s, 1H), 8.65 (s, 1H), 7.91 (d, $J = 12.9$ Hz, 1H), 7.58 (s, 1H), 6.57 (s, 1H), 4.89–4.80 (m, 1H), 4.18 (s, 1H), 3.81–3.61 (m, 8H), 1.38–1.19 (m, 7H). ^{13}C NMR (DMSO- d_6) δ : 176.3, 169.5, 165.9, 162.7, 153.9, 151.9, 148.1, 139.1, 118.9, 111.1, 110.9, 106.8, 66.5, 49.6, 49.2, 45.4, 44.5, 41.3, 35.9, 17.6, 7.6. HRMS m/z for $\text{C}_{22}\text{H}_{23}\text{Cl}_2\text{FN}_4\text{O}_5$ $[\text{M}+\text{H}]^+$ Calcd. 512.1025. Found: 513.1033

*(R),(S)*1-cyclopropyl-7-(4-((2,2-dichloroacetyl)alanyl)piperazin-1-yl)-6-fluoro-4-oxo-1,4-dihydroquinoline-3-carboxylic acid (DCA-DL-Ala-Cip, **8c**)

White microcrystals, m.p 216–218 °C, yield 57%. IR: $\nu_{\max}/\text{cm}^{-1}$ 3308, 3009, 2865, 1721, 1241, 1111, 804; ^1H NMR (DMSO- d_6) δ : 15.16 (s, 1H), 8.92 (s, 1H), 8.65 (s, 1H), 7.91 (d, $J = 12.7$ Hz, 1H), 7.58 (s, 1H), 6.57 (s, 1H), 4.91–4.79 (m, 1H), 4.39–4.32 (m, 1H), 3.81–3.62 (m, 8H), 1.32–1.19 (m, 7H). ^{13}C NMR (DMSO- d_6) δ : 176.3, 169.5, 165.9, 162.7, 152.0, 148.1, 145.0, 139.1, 119.1, 111.1, 111.0, 106.7, 66.5, 50.2, 49.6, 49.2, 45.4, 44.4, 36.0, 17.6, 7.6. HRMS m/z for $\text{C}_{22}\text{H}_{23}\text{Cl}_2\text{FN}_4\text{O}_5$ $[\text{M}+\text{H}]^+$ Calcd. 512.1025. Found: 513.1099

(R)-1-cyclopropyl-7-(4-((2,2-dichloroacetyl)-D-alanyl)piperazin-1-yl)-6-fluoro-4-oxo-1,4-dihydroquinoline-3-carboxylic acid (DCA-D-Ala-Cip, **8d**).

White microcrystals, m.p 204–206 °C, yield 77%. IR: $\nu_{\max}/\text{cm}^{-1}$ 3300, 3050, 2865, 1716, 1240, 1109, 803; ^1H NMR (DMSO- d_6) δ : 15.16 (s, 1H), 8.66 (s, 1H), 8.12 (s, 1H), 7.92 (d, J = 11.6 Hz, 1H), 7.58 (s, 1H), 6.58 (s, 1H), 4.88–4.80 (m, 1H), 4.53–4.41 (m, 1H), 3.82–3.55 (m, 8H), 1.37–1.19 (m, 7H). ^{13}C NMR (DMSO- d_6) δ : 176.4, 169.5, 165.9, 161.0, 152.0, 148.1, 145.0, 139.1, 119.0, 111.1, 111.0, 107.0, 66.5, 50.2, 49.1, 45.4, 44.4, 41.3, 36.0, 17.6, 7.6. HRMS m/z for $\text{C}_{22}\text{H}_{23}\text{Cl}_2\text{FN}_4\text{O}_5$ $[\text{M}+\text{H}]^+$ Calcd. 512.1030. Found: 513.1103

(S)-7-(4-((2,2-dichloroacetyl)isoleucyl)piperazin-1-yl)-1-ethyl-6-fluoro-4-oxo-1,4-dihydroquinoline-3-carboxylic acid (DCA-L-Ile-Cip, **8e**).

White microcrystals, m.p 212–214 °C, yield 83%. IR: $\nu_{\max}/\text{cm}^{-1}$ 3200, 3000, 2968, 1712, 1256, 1112, 804; ^1H NMR (DMSO- d_6) δ : 15.16 (s, 1H), 8.89–8.88 (m, 1H), 8.65 (s, 1H), 7.91 (d, J = 12.5 Hz, 1H), 7.58 (s, 1H), 6.61 (s, 1H), 4.85–4.72 (m, 2H), 3.82–3.61 (m, 8H), 1.46–0.85 (m, 13H). ^{13}C NMR (DMSO- d_6) δ : 176.3, 168.8, 165.9, 163.4, 151.9, 148.0, 144.7, 139.1, 118.9, 111.1, 110.9, 106.8, 66.4, 53.0, 49.7, 49.3, 45.5, 44.0, 36.7, 35.9, 23.7, 15.5, 11.0, 7.6. HRMS m/z for $\text{C}_{25}\text{H}_{29}\text{Cl}_2\text{FN}_4\text{O}_5$ $[\text{M}+\text{Na}]^+$ Calcd. 577.1391. Found: 577.1373

(S)-1-cyclopropyl-7-(4-((2,2-dichloroacetyl)valyl)piperazin-1-yl)-6-fluoro-4-oxo-1,4-dihydroquinoline-3-carboxylic acid (DCA-L-Val-Cip, **8f**).

White microcrystals, m.p 241–243 °C, yield 74%. IR: $\nu_{\max}/\text{cm}^{-1}$ 3280, 3050, 2931, 1709, 1239, 1114, 804; ^1H NMR (DMSO- d_6) δ : 15.18 (s, 1H), 8.83 (d, J = 9.4 Hz, 1H), 8.68 (s, 1H), 7.94 (d, J = 13.1 Hz, 1H), 7.59 (d, J = 8.1 Hz, 1H), 6.63 (s, 1H), 4.74–4.69 (m, 1H), 3.82–3.61 (m, 7H), 2.10–2.03 (m, 1H), 1.33–1.19 (m, 6H), 0.92–0.87 (m, 6H). ^{13}C NMR (DMSO- d_6) δ : 176.3, 168.7, 165.8, 163.5, 151.9, 148.0, 144.8, 139.1, 118.9, 111.1, 110.9, 106.7, 66.4, 53.8, 49.7, 49.3, 45.3, 45.0, 35.9, 30.5, 19.3, 17.4, 7.6. HRMS m/z for $\text{C}_{24}\text{H}_{27}\text{Cl}_2\text{FN}_4\text{O}_5$ $[\text{M}+\text{H}]^+$ Calcd. 540.1341. Found: 541.1413

(S)-1-cyclopropyl-7-(4-((2,2-dichloroacetyl)phenylalanyl)piperazin-1-yl)-6-fluoro-4-oxo-1,4-dihydroquinoline-3-carboxylic acid (DCA-L-Phe-Cip, **8g**).

White microcrystals, m.p 153–155 °C, yield 67%. IR: $\nu_{\max}/\text{cm}^{-1}$ 3220, 3008, 2980, 1719, 1256, 1111, 805; ^1H NMR (DMSO- d_6) δ : 15.18 (br s, 1H), 9.11 (s, 1H), 8.65 (s, 1H), 8.42 (s, 1H), 7.88 (d, J = 13.2 Hz, 1H), 7.48–7.21 (m, 5H), 6.55 (s, 1H), 5.1–4.99 (m, 1H), 4.77–4.70 (m, 1H), 3.81–2.91 (m, 10H), 1.33–1.19 (m, 4H). ^{13}C NMR (DMSO- d_6) δ : 176.3, 168.4, 165.9, 163.0, 151.9, 148.1, 144.7, 139.1, 129.9, 129.6, 128.7, 128.2, 126.7, 118.9, 111.1, 110.9, 106.7, 66.3, 50.3, 49.1, 45.4, 44.7, 41.2, 37.5, 35.9, 8.5, 7.6. HRMS m/z for $\text{C}_{28}\text{H}_{27}\text{Cl}_2\text{FN}_4\text{O}_5$ $[\text{M}+\text{H}]^+$ Calcd. 588.1338. Found: 589.1408

*(S)*7-(4-((2,2-dichloroacetyl)glycyl)piperazin-1-yl)-1-ethyl-6-fluoro-4-oxo-1,4-dihydroquinoline-3-carboxylic acid (DCA-Gly-Nor, **9a**).

White microcrystals, m.p 242–244 °C, yield 62%. IR: $\nu_{\max}/\text{cm}^{-1}$ 3383, 3052, 2923, 1720, 1244, 1111, 808; ^1H NMR (DMSO- d_6) δ : 15.32 (s, 1H), 8.97 (s, 1H), 8.72 (s, 1H), 7.94 (d, J = 12.8 Hz, 1H), 7.20 (s, 1H), 6.69 (s, 1H), 4.63–4.57 (m, 2H), 4.18–4.13 (m, 2H), 3.69–3.65 (m, 4H), 3.38–3.33 (m, 4H), 1.45–1.39 (m, 3H). ^{13}C NMR (DMSO- d_6) δ : 176.2, 166.1, 163.8, 163.7, 151.8, 148.6, 145.2, 137.1, 119.9, 111.3, 106.8, 106.2, 66.5, 49.5, 49.4, 49.2, 49.1, 43.8, 41.2, 14.4. HRMS m/z for $\text{C}_{20}\text{H}_{21}\text{Cl}_2\text{FN}_4\text{O}_5$ $[\text{M}+\text{H}]^+$ Calcd. 486.0867. Found: 487.0947

*(S)*7-(4-((2,2-dichloroacetyl)-L-alanyl)piperazin-1-yl)-1-ethyl-6-fluoro-4-oxo-1,4-dihydroquinoline-3-carboxylic acid (DCA-L-Ala-Nor, **9b**).

White microcrystals, m.p 256–258 °C, yield 85%. IR: $\nu_{\max}/\text{cm}^{-1}$ 3301, 3050, 2927, 1706, 1239, 1111, 804; ^1H NMR (DMSO- d_6) δ : 15.32 (s, 1H), 8.97–8.91 (m, 2H), 7.94 (d, J = 11.9 Hz, 1H), 7.21 (s, 1H), 6.57 (s, 1H), 4.88–4.80 (m, 1H), 4.64–4.55 (m, 2H), 3.74–3.67 (m, 8H), 1.42–1.40 (m, 3H), 1.27–1.23 (m, 3H). ^{13}C NMR (DMSO- d_6) δ : 176.2, 169.5, 166.1, 162.7, 153.8, 151.9, 148.6, 145.1, 137.1, 111.4, 111.2, 107.1, 106.3, 66.4, 49.7, 49.3, 49.1, 45.4, 44.6, 17.7, 14.4. HRMS m/z for $\text{C}_{21}\text{H}_{23}\text{Cl}_2\text{FN}_4\text{O}_5$ $[\text{M}+\text{H}]^+$ Calcd. 523.0922. Found: 523.0917

*(R)*7-(4-((2,2-dichloroacetyl)-D-alanyl)piperazin-1-yl)-1-ethyl-6-fluoro-4-oxo-1,4-dihydroquinoline-3-carboxylic acid (DCA-D-Ala-Nor, **9c**).

White microcrystals, m.p 237–239 °C, yield 78%. IR: $\nu_{\max}/\text{cm}^{-1}$ 3308, 3050, 2930, 1708, 1241, 1111, 804; ^1H NMR (DMSO- d_6) δ : 15.30 (br s, 1H), 8.95–8.91 (m, 2H), 7.93 (d, J = 15.5 Hz, 1H), 7.21 (s, 1H), 6.57 (s, 1H), 4.63–4.54 (m, 2H), 4.88–4.80 (m, 1H), 3.74–3.48 (m, 8H), 1.44–

1.39 (m, 3H), 1.26 (d, $J = 5.0$ Hz, 3H). ^{13}C NMR (DMSO- d_6) δ : 176.2, 169.5, 166.1, 162.8, 151.8, 148.6, 145.1, 137.1, 119.6, 111.3, 107.1, 106.3, 66.5, 49.7, 49.1, 45.4, 44.6, 42.4, 41.3, 17.7, 14.4. HRMS m/z for $\text{C}_{21}\text{H}_{23}\text{Cl}_2\text{FN}_4\text{O}_5$ $[\text{M}+\text{H}]^+$ Calcd. 500.1024. Found: 501.11

*(S)*7-(4-((2,2-dichloroacetyl)isoleucyl)piperazin-1-yl)-1-ethyl-6-fluoro-4-oxo-1,4-dihydroquinoline-3-carboxylic acid (DCA-I-Ile-Nor, **9d**)

White microcrystals, m.p 219–221 °C, yield 75%. IR: $\nu_{\text{max}}/\text{cm}^{-1}$ 3269, 3050, 2980, 1687, 1241, 1117, 805; ^1H NMR (DMSO- d_6) δ : 15.30 (br s, 1H), 8.94–8.89 (m, 2H), 7.90 (d, $J = 10$ Hz, 1H), 7.44 (s, 1H), 6.63 (s, 1H), 4.72–4.59 (m, 3H), 3.82–3.36 (m, 8H), 1.84 (s, 1H), 1.58–1.30 (m, 3H), 1.20–0.86 (m, 8H). ^{13}C NMR (DMSO- d_6) δ : 176.1, 168.8, 166.1, 163.4, 151.8, 148.5, 145.0, 137.1, 119.5, 111.3, 107.1, 106.2, 66.4, 53.0, 52.9, 49.4, 49.1, 45.4, 45.0, 36.8, 23.7, 15.5, 14.4, 11.0. HRMS m/z for $\text{C}_{24}\text{H}_{29}\text{Cl}_2\text{FN}_4\text{O}_5$ $[\text{M}+\text{H}]^+$ Calcd. 542.1482. Found: 543.1562

*(S)*7-(4-((2,2-dichloroacetyl)valyl)piperazin-1-yl)-1-ethyl-6-fluoro-4-oxo-1,4-dihydroquinoline-3-carboxylic acid (DCA-L-Val-Nor **9e**).

White microcrystals, m.p 240–242 °C, yield 76%. IR: $\nu_{\text{max}}/\text{cm}^{-1}$ 3280, 3050, 2931, 1688, 1234, 1112, 806.; ^1H NMR (DMSO- d_6) δ : 15.30 (brs, 1H), 8.96 (s, 1H), 8.82 (d, $J = 7.1$ Hz, 1H), 7.94 (d, $J = 12.3$ Hz, 1H), 7.21 (s, 1H), 6.64 (s, 1H), 4.75–4.69 (m, 1H), 4.63–4.55 (m, 2H), 3.81–3.72 (m, 8H), 2.10–2.01 (m, 1H), 1.44–1.39 (m, 3H), 0.91–0.88 (m, 6H). ^{13}C NMR (DMSO- d_6) δ : 176.2, 168.7, 166.1, 163.4, 151.8, 148.6, 145.1, 137.1, 119.6, 111.3, 107.1, 106.3, 66.4, 54.0, 53.8, 49.8, 49.4, 49.1, 45.0, 30.6, 19.3, 17.4, 14.4. HRMS m/z for $\text{C}_{23}\text{H}_{27}\text{Cl}_2\text{FN}_4\text{O}_5$ $[\text{M}+\text{H}]^+$ Calcd. 528.1341. Found: 529.1416

*(S)*7-(4-((2,2-dichloroacetyl)phenylalanyl)piperazin-1-yl)-1-ethyl-6-fluoro-4-oxo-1,4-dihydroquinoline-3-carboxylic acid (DCA-L-Phe-Nor, **9f**).

White microcrystals, m.p 114–116 °C, yield 64%. IR: $\nu_{\text{max}}/\text{cm}^{-1}$ 3220, 3029, 2980, 1697, 1240, 1113, 807; ^1H NMR (DMSO- d_6) δ : 15.30 (br s, 1H), 9.10 (s, 1H), 8.95 (s, 1H), 7.90 (d, $J = 11$ Hz, 1H), 7.43–7.04 (m, 6H), 6.55 (s, 1H), 5.04–4.98 (m, 1H), 4.57–4.54 (m, 2H), 3.68–2.73 (m, 10H), 1.47–1.32 (m, 3H). ^{13}C NMR (DMSO- d_6) δ : 176.2, 168.4, 166.1, 163.0, 151.8, 148.6, 145.0, 137.1, 136.5, 129.5, 129.3, 128.4, 128.2, 126.7, 111.3, 111.2, 107.1, 106.1, 66.3, 50.3, 49.3, 49.1, 45.4, 44.7, 41.3, 37.5, 14.4. HRMS m/z for $\text{C}_{27}\text{H}_{27}\text{Cl}_2\text{FN}_4\text{O}_5$ $[\text{M}+\text{H}]^+$ Calcd. 576.1335. Found: 577.141

1-Cyclopropyl-7-(4-(2,2-dichloroacetyl)piperazin-1-yl)-6-fluoro-4-oxo-1,4-dihydroquinoline-3-carboxylic acid (DCA-Cip, 15).

Yellow microcrystals, m.p 250–252 °C, yield 88%. IR: $\nu_{\max}/\text{cm}^{-1}$ 3017, 2865, 1720, 1245, 1097, 804; ^1H NMR (DMSO- d_6) δ : 15.17 (s, 1H), 8.66 (s, 1H), 7.93 (d, $J = 12.4$ Hz, 1H), 7.33 (s, 1H), 6.41 (s, 1H), 3.81–3.54 (m, 9H), 1.31–1.19 (m, 4H). ^{13}C NMR (DMSO- d_6) δ : 176.4, 165.9, 161.9, 151.9, 148.2, 148.1, 139.1, 119.0, 111.2, 106.8, 99.5, 65.8, 49.2, 48.9, 42.6, 42.3, 35.9, 7.6. HRMS m/z for $\text{C}_{19}\text{H}_{18}\text{Cl}_2\text{FN}_3\text{O}_4$ $[\text{M}+\text{H}]^+$ Calcd. 441.0658. Found: 441.0689

7-(4-(2,2-dichloroacetyl)piperazin-1-yl)-1-ethyl-6-fluoro-4-oxo-1,4-dihydroquinoline-3-carboxylic acid (DCA-Nor, 16).

Yellow microcrystals, m.p 220–222°C, yield 63%. IR: $\nu_{\max}/\text{cm}^{-1}$ 3017, 2931, 1713, 1240, 1110, 804; ^1H NMR (DMSO- d_6) δ : 15.29 (br s, 1H), 8.94 (s, 1H), 7.90 (d, $J = 12.4$ Hz, 1H), 7.33 (s, 1H), 6.40 (s, 1H), 4.63–4.52 (m, 2H), 3.78–3.54 (m, 8H), 1.45–1.33 (m, 3H). ^{13}C NMR (DMSO- d_6) δ : 176.1, 166.1, 161.9, 151.8, 148.6, 144.9, 137.1, 119.6, 111.3, 107.1, 106.4, 65.8, 49.3, 49.1, 45.3, 42.6, 42.4, 14.4. HRMS m/z for $\text{C}_{18}\text{H}_{18}\text{Cl}_2\text{FN}_3\text{O}_4$ $[\text{M}+\text{H}]^+$ Calcd. 429.0658. Found: 429.0678

Biological studies

Antimicrobial properties

Methodology of the antimicrobial activity determination is mentioned in the supplementary material.

Antiproliferative properties

Methodology of the antiproliferative properties of the synthesized compounds against RPE1 cell line is mentioned in the supplementary material.

***E-coli* DNA gyrase inhibitory properties**

Methodology of the *E. coli* DNA gyrase inhibitory properties of the tested compounds is mentioned in the supplementary material.

2D-QSAR studies

Methodology of the 2D-QSAR studies is mentioned in the supplementary material

Results and discussion

Chemistry

N-Acylbenzotriazoles are efficient reagents for acylation reactions (Panda et al., 2014). The carboxyl group of dichloroacetic acid **1** was activated by a modified reported procedure. The synthesis of benzotriazolide of dichloroacetic acid **3** was reported by Katritzky *et al* (Katritzky et al., 2003). However, we were unable to get the product by following the described procedure. After several trials, we observed that the compound is not stable in basic conditions. So we modified the method from basic workup to acidic workup. The advantage of benzotriazole chemistry is the accessibility to use either acid or base to remove the excess benzotriazole from the reaction mixture.

DCA hybrid conjugates with antibiotics and amino acid as linker were prepared by using two different routes. In route I, the benzotriazolide of dichloroacetic acid **3** was treated with amino acids **4** in the presence of triethylamine in the acetonitrile-water mixture. We were unable to activate the DCA-amino acid conjugate by using benzotriazole chemistry. To prepare our target hybrid conjugates we explored different coupling reagents like HOBt, EDC and DCC. Every time we confirmed the formation of the product **8** by NMR but in the impure form (Scheme 1). We also failed to purify the hybrid conjugates by column chromatography. We switched to an alternative synthetic route.

Insert Scheme 1

In route II, we utilized Boc protected amino acid–fluoroquinolone conjugates **11a–g** and **12a–f** prepared by our previously reported method (Panda et al., 2014). Boc group deprotection with dioxane/HCl mixture at 20 °C for 2 h gave the unprotected amino acid–fluoroquinolone conjugates, which were further used for the next step without characterization. The target hybrid conjugates **8a–g** and **9a–f** were prepared by coupling unprotected amino acid–fluoroquinolone

conjugates with DCA–benzotriazolide **3** in the presence of triethylamine at 20 °C for 4-6 h in good yields (31–77%) (Scheme 2).

Insert Scheme 2

To better understand the importance of amino acid in these hybrid conjugates, we have also synthesized DCA-fluoroquinolone conjugates without any linker. The DCA-benzotriazole **3** was treated with the ciprofloxacin **6** and norfloxacin **7** under microwave irradiation in the presence of TEA to obtain the conjugates in good yields (Scheme 3)

Insert Scheme 3

Biological studies

Antimicrobial properties

Antimicrobial properties of the synthesized hybrid conjugates **8a–g**, **9a–f**, **15** and **16** were determined by the standard techniques and compared with the parent fluoroquinolone antibiotics **6** and **7** (Clinical & Laboratory Standards Institute, 2012). The antimicrobial properties of the tested conjugates and their standard precursors (**6**, **7**) against Gram-negative (*E. coli*, *P. aeruginosa*) and Gram-positive (*S. aureus*, *E. faecalis*) bacteria were determined in MIC (μM) values (Table 1).

From the observed data, it has been noticed that the parent antibiotics show antimicrobial properties with higher potency against the tested Gram-negative bacteria relative to the Gram-positive strains. Considering that ciprofloxacin **6** is of higher efficacy/potency than norfloxacin **7** (MIC = 0.377, 6.263; 5.030, 12.526, 12.072, 83.506; 24.144, 100.207 μM for **6** and **7** against *E. coli*, *P. aeruginosa*, *S. aureus*, and *E. faecalis*, respectively). The synthesized hybrid conjugates **8c** and **8d** reveal enhanced antimicrobial properties against three of the tested microorganisms with potency 1.9, 61.9, 20.7 and 2.4, 37.1, 8.3 folds relative to the parent precursor antibiotic **6** against *E. coli*, *S. aureus* and *E. faecalis*, respectively. Compound **15** also reveals remarkable antimicrobial properties with potency 5.5, 1.1, 42.7 and 9.2 folds relative to the antibiotic **6** against *E. coli*, *P. aeruginosa*, *S. aureus*, and *E. faecalis*, respectively. It has also been noticed that the D-amino acid bearing conjugates are of higher antimicrobial properties than the L-analogues as exhibited in pairs **8b/8d** and **9b/9c**. We also observed phenylalanine containing conjugates are less

active compared to others. For better understanding, the SAR (structure-activity relationships), computational studies were considered.

Antiproliferative properties

Antiproliferative properties of the synthesized conjugates (**8a–g**, **9a–f**, **15** and **16**) were determined by the standard MTT technique utilizing RPE1 (normal human immortalized retinal epithelial) cell line (Ismail et al., 2016). Table S1 (Supplementary material) reveals that all the synthesized conjugates reveal safe profile (antiproliferation < 20%) against the tested normal human cell line utilized at 100 μ M (% of cell proliferation = 98.2–80.0). This observation may support the safe application of the synthesized compounds.

***E-coli* DNA gyrase inhibitory properties**

DNA replication, transcription, and other cellular transactions usually initiated by uncoiling and unwinding DNA helices. The DNA helices are super-coiled inside the cell. Topoisomerase enzymes are responsible for the DNA topological steps (Badshah & Ullah, 2018). Two main types of topoisomerases are well known. Type-I catalyzes single DNA strand break while type-II (gyrase) capable for break two DNA strands at single circular and twisted around each other i.e. removing the links in the DNA replication forks (Tiz et al., 2019; Ponnusamy et al., 2018; Gençer et al., 2017). DNA gyrase is a famous drug discovery target for developing antibacterial active agents due to the negative DNA super-coiling effect capable to block DNA replication and eventually bacterial cell death (Tomašič et al., 2017; Zhang et al., 2016). Fluoroquinolones are well-known DNA gyrase inhibitors in many bacterial species (Towle et al., 2018; Carta et al., 2019).

The conjugates synthesized revealing potent antimicrobial properties against *E. coli* (**8c**, **8d** and **15**) were subjected for DNA gyrase supercoiling bioassay and the data compared with that of their parent antibiotic, ciprofloxacin (CIP). The study can validate the observed antimicrobial properties and also reveal the selectivity towards the targeted enzyme (mode of action). From the results obtained (Table 2, Fig. 2) it can be concluded that CIP seems the most effective/selective agent towards the targeted enzyme relative to the other tested conjugates ($IC_{50} = 2.27 \mu$ M). Conjugate **8c** reveals higher potency/selectivity (about 3 folds) than **8d** ($IC_{50} = 3.25, 9.80 \mu$ M for **8c** and **8d**, respectively). Also, compound **15** reveals promising efficacy towards the targeted enzyme with lower potency/selectivity than the parent antibiotic CIP ($IC_{50} = 3.55 \mu$ M, 64%

relative efficacy to CIP). We believe there must be an additional mechanism responsible for the activity of the conjugates and we assume DCA must be playing an important role in inhibiting pyruvate dehydrogenase kinase. Based on a report from 2012 by Birkenstock *et al.*, pyruvate dehydrogenase is an important target for antibiotics (Birkenstock *et al.*, 2012).

Insert Fig. 2

2D-QSAR studies

The conjugates synthesized with variable antimicrobial properties against *E. coli*, *S. aureus* and *E. faecalis* were subjected for 2D-QSAR studies to better understand the factors affecting/controlling the biological properties. The QSAR models (CODESSA-Pro software) (Srour *et al.*, 2018), as well as an explanation of their descriptors, are mentioned in the supplementary material (Tables S2–S10, Figs. S1–S3). The estimated antimicrobial properties due to the QSAR models are close to the experimental values. Additionally, the statistical parameters (including cross-validation leave one-out and many-out “up to 20% of the training set” correlation coefficients) of the QSAR models support their goodness for utilization in predication of effective hits ($R^2 = 0.924, 0.958, 0.962$; $R^2_{cvOO} = 0.870, 0.923, 0.928$; $R^2_{cvMO} = 0.886, 0.928, 0.936$ for *E. coli*, *S. aureus* and *E. faecalis*, respectively).

Conclusions

A set of dichloroacetic acid-fluoroquinolone conjugates **8a–g**, **9a–f**, **15** and **16** were synthesized in good yields using benzotriazole chemistry. The synthesized compounds were bio-assayed against Gram positive and Gram negative pathogens following the in vitro standard procedure. Some of the synthesized hybrids exhibited antibacterial properties with higher potency than the starting precursor, fluoroquinolones (used as standard reference). Conjugates **8c** and **8d** revealed antimicrobial properties against with potency 1.9, 61.9, 20.7 and 2.4, 37.1, 8.3 folds relative to the parent antibiotic **6** against *E. coli*, *S. aureus* and *E. faecalis*, respectively. Also, compound **15** revealed promising antimicrobial properties with potency 5.5, 1.1, 42.7 and 9.2 folds relative to **6** against *E. coli*, *P. aeruginosa*, *S. aureus*, and *E. faecalis*, respectively. The DNA gyrase enzymatic study supports the experimental data. We believe there is more than one mode of mechanisms are involved in the antibacterial property of the conjugates. 2D-QSAR is explored in the present study for validating the observed data and determining the most important

structural parameters responsible for the properties. A robust BMLR-QSAR model developed for the antibacterial activities using CODESSA-Pro software.

Acknowledgments

We thank the Egyptian Cultural and Educational Bureau Scholarship. Authors also thank the Center for Undergraduate Research and Scholarship (CURS) and Translational Research Program (TRP) at Augusta University for financial support.

Conflict of interest

The authors state no conflict interest.

Data Availability Statement

All data generated or analyzed during this study are included in this published article and its Supplementary Information Files.

Figure Legends

Fig. 1. Examples of different class of antibiotics.

Scheme 1. Route I for the synthesis of hybrid conjugates **8a–g** and **9a–f**.

Scheme 2. Route II for the synthesis of hybrid conjugates.

Scheme 3. Synthesis of DCA-ciprofloxacin and DCA-norfloxacin conjugates.

Fig. 2. Preview depicting the *E. coli* DNA gyrase supercoiling assay of CIP, conjugates **8c**, **8d** and **15** at different concentrations (0.1, 1, 10, and 100 μ M).

References

- Allaka, T. R., Polkam, N., Rayam, P., Sridhara, J., Garikapati, N. S., Kotapalli, S. S., Ummanni, R., & Anireddy, J. S. (2016). Design, synthesis and biological activity evaluation of novel pefloxacin derivatives as potential antibacterial agents. *Med Chem Res.*, 25(5), 977–993.
- Badshah, S. L., & Ullah, A. (2018). New developments in non-quinolone-based antibiotics for the inhibition of bacterial gyrase and topoisomerase IV. *Eur. J. Med. Chem.*, 152, 393–400.
- Balaban, N.Q., Levin-Reisman, I., Ronin, I., Gefen, O., Shores, N., & Braniss, I. (2017). Antibiotic tolerance facilitates the evolution of resistance. *Science*, 355(6327), 826–830.

- Bartzatt, R., Cirillo, S. L. G., & Cirillo, J. D. (2013). Antibacterial derivatives of ciprofloxacin to inhibit growth of necrotizing fasciitis associated penicillin resistant *Escherichia coli*. *J Pharm.*, 2013, 1–7.
- Birkenstock, T., Liebeke, M., Winstel, V., Krismer, B., Gekeler, C., Niemiec, M. J., Bisswanger, H., Lalk, M., Peschel, A. (2012) Exometabolome analysis identifies pyruvate dehydrogenase as a target for the antibiotic triphenylbismuthdichloride in multiresistant bacterial pathogens. *J. Biol. Chem.*, 287, 2887–2895.
- Brown, E. D., & Wright, G.D. (2016). Antibacterial drug discovery in the resistance era. *Nature*, 529, 336–343.
- Carta, A., Bua, A., Corona, P., Piras, S., Briguglio, I., Molicotti, P., Zanetti, S., Laurini, E., Aulic, S., Fermeglia, M., & Pricl, S. (2019). Design, synthesis and antitubercular activity of 4-alkoxytriazoloquinolones able to inhibit the *M. tuberculosis* DNA gyrase. *Eur. J. Med. Chem.*, 161, 399–415.
- Casini, G., Ferappi, M., & Grifantini, M. (1966). Dichloroacetic acid derivatives with antibacterial activity. II. Dichloroacetyl derivatives and aziridine derivatives of substances with quinone structure. *Farmaco Sci.*, 21(2), 861–869.
- Clinical and Laboratory Standards Institute. Methods for Dilution Antimicrobial Susceptibility Tests for Bacteria That Grow Aerobically; Approved Standard—Ninth Edition. CLSI document M07-A9. Clinical and Laboratory Standards Institute, Wayne, Pennsylvania, USA, 2012.
- Faidallah, H. M., Girgis, A. S., Tiwari, A. D., Honkanadavar, H. H., Thomas, S. J., Samir, A., Kalmouch, A., Alamry, K. H., Khalid, A., Khan, K. A., Ibrahim, T. S., AL-Mahmoudy, A. M. M., Asiri, A. M., & Panda, S. S. (2018). Synthesis, antibacterial properties and 2D-QSAR studies of quinolone-triazole conjugates. *Eur J Med Chem.*, 143, 1524–1534.
- Florio, R., De Lellis, L., Veschi, S., Verginelli, F., Giacomo, V., Gallorini, M., Perconti, S., Sanna, M., Costantini, R. M., Natale, A., Arduini, A., Amoroso, R., Cataldi, A., & Cama, A. (2018). Effects of dichloroacetate as single agent or in combination with GW6471 and metformin in paraganglioma cells. *Sci Rep.*, 8(13610), 1–14.
- Gençer, H. K., Levent, S., Çevik, U. A., Özkay, Y., & Ilgın, S. (2017). New 1, 4-dihydro[1,8]naphthyridine derivatives as DNA gyrase inhibitors. *Bioorg. Med. Chem. Lett.*, 27(5), 1162–1168.

- Ibrahim, M. A., Panda, S. S., Birs, A. S., Juan, C., Serrano, J. C., Gonzalez, C. F., Alamry, K. A., & Katritzky, A. R. (2014). Synthesis and antibacterial evaluation of amino acid-antibiotic conjugates. *Bioorganic Med Chem Lett.*, 24(7), 1856–1861.
- Ismail, N. S. M., George, R. F., Serya, R. A. T., Baseliious, F. N., El-Manawaty, M., Shalaby, E. M., & Girgis, A. S. N. (2016). Rational design, synthesis and 2D-QSAR studies of antiproliferative tropane-based compounds. *RSC Advances*, 6(104), 101911–101923.
- Katritzky, A. R., Zhang, Y., & Singh, S. K. (2003). Efficient conversion of carboxylic acids into *N*-acylbenzotriazoles. *Synthesis*, 18, 2795–2798.
- Panda, S. S., Detistov, O. S., Girgis, A. S., Mohapatra, P. P., Samir, A., & Katritzky, A. R. (2016). Synthesis and molecular modeling of antimicrobial active fluoroquinolone-pyrazine conjugates with amino acid linkers. *Bioorganic Med Chem Lett.*, 26(9), 2198–2205.
- Panda, S. S., Hall, C. D., Oliferenko, A. A., & Katritzky, A. R. (2014). Traceless chemical ligation from S -, O -, and N-acyl isopeptides. *Acc Chem Res.*, 47(4), 1076–1081
- Panda, S. S., Liaqat, S., Girgis, A. S., Samir, A., Hall, C. D., & Katritzky, A. R. (2015). Novel antibacterial active quinolone-fluoroquinolone conjugates and 2D-QSAR studies. *Bioorganic Med Chem Lett.*, 25(18), 3816–3821.
- Panda, S. S., Naumov, R. N., Asiri, A. M., & Katritzky, A. R. (2014). Microwave-assisted synthesis of biotin conjugates with quinolone antibiotics via amino acids. *Synthesis*, 46(11), 1511–1517
- Peleg, A.Y., & Hooper, D.C. (2010). Hospital-acquired infections due to Gram-negative bacteria. *N Engl J Med.*, 362, 1804–1813.
- Ponnusamy, T., Alagumuthu, M., & Thamaraiselvi, S. (2018). Drug efficacy of novel 3-O-methoxy-4-halo disubstituted 5,7-dimethoxy chromans; evaluated via DNA gyrase inhibition, bacterial cell wall lesion and antibacterial prospective. *Bioorg. Med. Chem.*, 26(12), 3438–3452.
- Rajulu, G. G., Naik, H. S. B., Kumar, G. C., Ramaraj, S., Sambasivam, G., & Koppolu, K. P. (2014). New azetidine-3-carbonyl-N-methyl-hydrazino derivatives of fluoroquinolones: Synthesis and evaluation of antibacterial and anticancer properties. *Med Chem Res.*, 23(6), 2856–2868.
- Sarro, D. A., & Sarro, D. G. (2001). Adverse Reactions to fluoroquinolones. An overview on mechanistic aspects. *Curr. Med. Chem.*, 8(4), 371–384.

- Silver, L. L. (2011). Challenges of antibacterial discovery. *Clinical Microbiology Rev.*, 24(1), 71–109.
- Sprenger, M., & Fukuda, K. (2016). New mechanisms, new worries. *Science*, 351(6279), 1263–1264.
- Srouf, A. M., Panda, S. S., Salman A. M. M., El-Manawaty, M. A., George, R. F., Shalaby, E. M., Fitch, A. N., Fawzy, N. G., & Girgis, A. S. (2018). Synthesis and molecular modeling studies of bronchodilatory active indole-pyridine conjugates. *Future Med. Chem.*, 10(15), 1787–1804.
- Sutendra, G., & Michelakis, E. D. (2013). Pyruvate dehydrogenase kinase as a novel therapeutic target in oncology. *Front Oncol.*, 3(38), 1–11.
- Tiwari, A. D., Panda, S. S., Asiri, A. M., Hall, C. D., & Katritzky, A. R. (2014). Fluorescent-labeled Amino acid-Antibiotic Conjugates. *Synthesis*, 46(18), 2430–2435.
- Tiz, D. B., Skok, Z., Durcik, M., Tomašič, T., Mašič, L. P., Ilaš, J., Zega, A., Draskovits, G., Révész, T., Nyerges, A., Pál, C., Cruz, C. D., Tammela, P., Žigon, D., Kikelj, D., & Zidar, N. (2019). An optimised series of substituted *N*-phenylpyrrolamides as DNA gyrase B inhibitors. *Eur. J. Med. Chem.*, 167, 269–290.
- Tomašič, T., Mirt, M., Barančoková, M., Ilaš, J., Zidar, N., Tammela, P., & Kikelj, D. (2017). Design, synthesis and biological evaluation of 4,5-dibromo-*N*-(thiazol-2-yl)-1*H*-pyrrole-2-carboxamide derivatives as novel DNA gyrase inhibitors. *Bioorg. Med. Chem.*, 25(1), 338–349.
- Towle, T. R., Kulkarni, C. A., Opegard, L. M., Williams, B. P., Picha, T. A., Hiasa, H., & Kerns, R. J. (2018). Design, synthesis, and evaluation of novel N-1 fluoroquinolone derivatives: Probing for binding contact with the active site tyrosine of gyrase. *Bioorg Med Chem Lett.*, 28(10), 1903–1910.
- Zhang, L., Addla, D., Ponmani, J., Wang, A., Xie, D., Wang, Y. N., Zhang, S. L., Geng, R. X., Cai, G. X., Li, S., & Zhou, C. H. (2016). Discovery of membrane active benzimidazole quinolones-based topoisomerase inhibitors as potential DNA-binding antimicrobial agents. *Eur. J. Med. Chem.*, 111, 160–182.
- Zhang, T., Wu, J., Chen, S., Liu, K., Lin, Y., Guo, H., & Liu, M. (2014). Synthesis and antibacterial activity of amino acid and dipeptide prodrugs of IMB-070593, a fluoroquinolone candidate. *Molecules*, 19(5), 6822–6837.

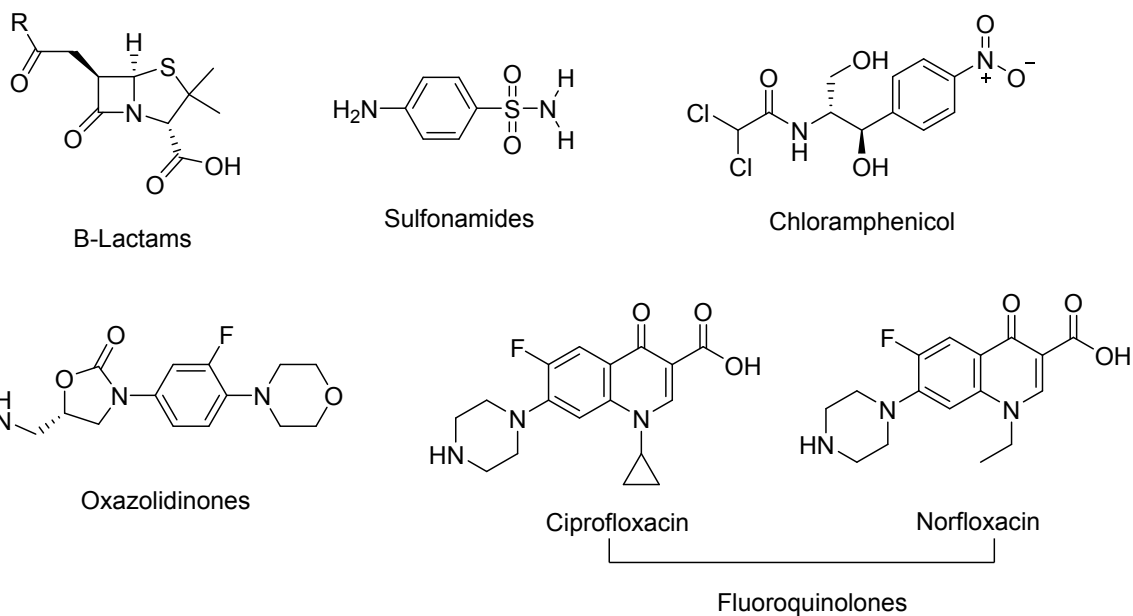
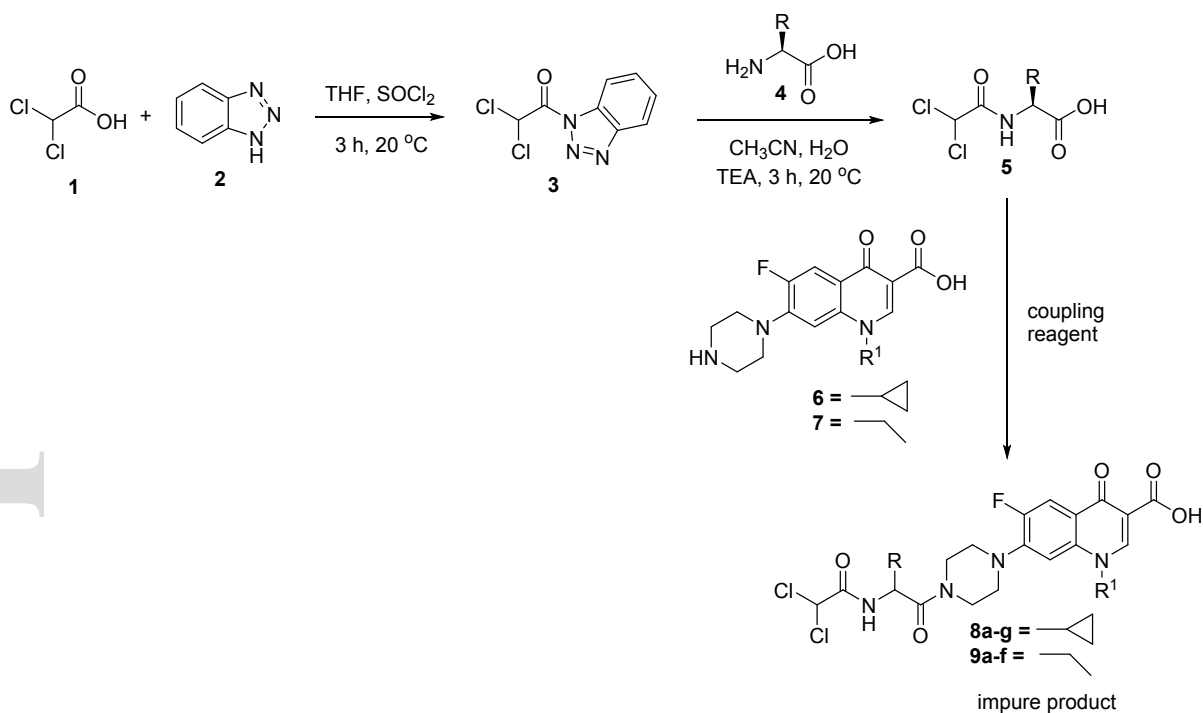
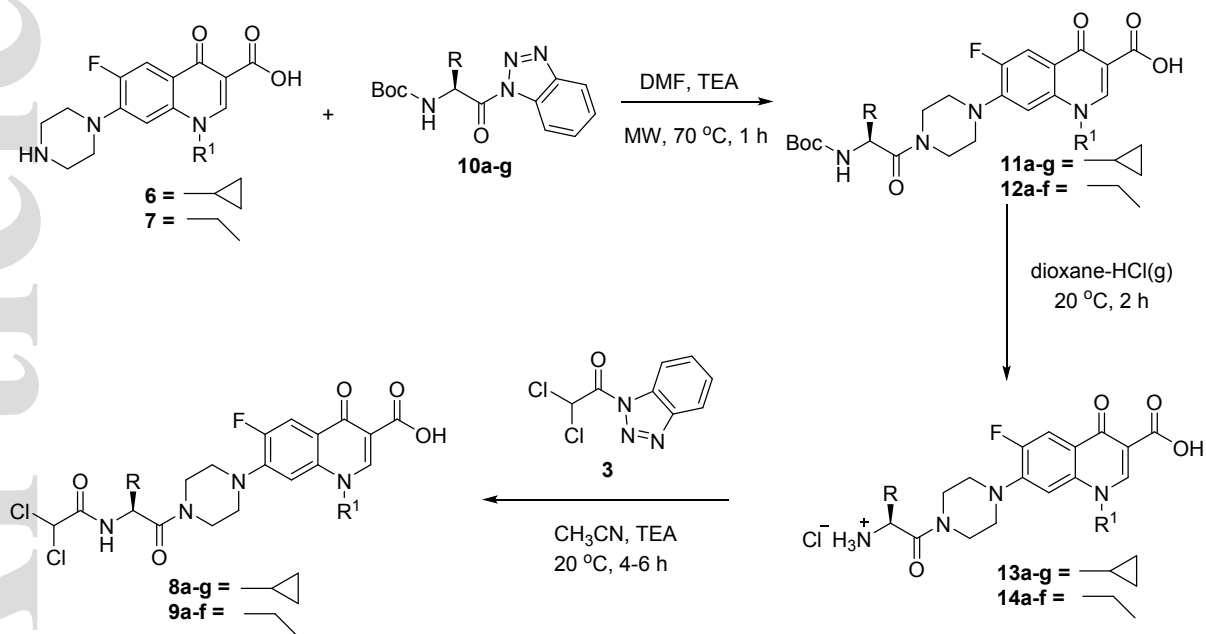


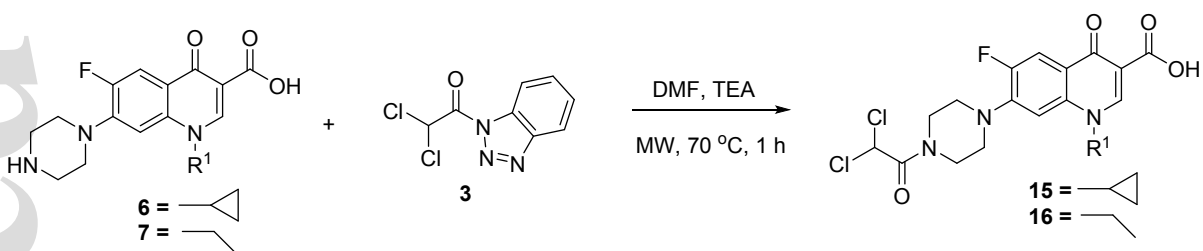
Fig. 1. Examples of different class of antibiotics.



Scheme 1. Route I for the synthesis of hybrid conjugates **8a–g** and **9a–f**.



Scheme 2. Route II for the synthesis of hybrid conjugates.



Scheme 3. Synthesis of DCA-ciprofloxacin and DCA-norfloxacin conjugates.

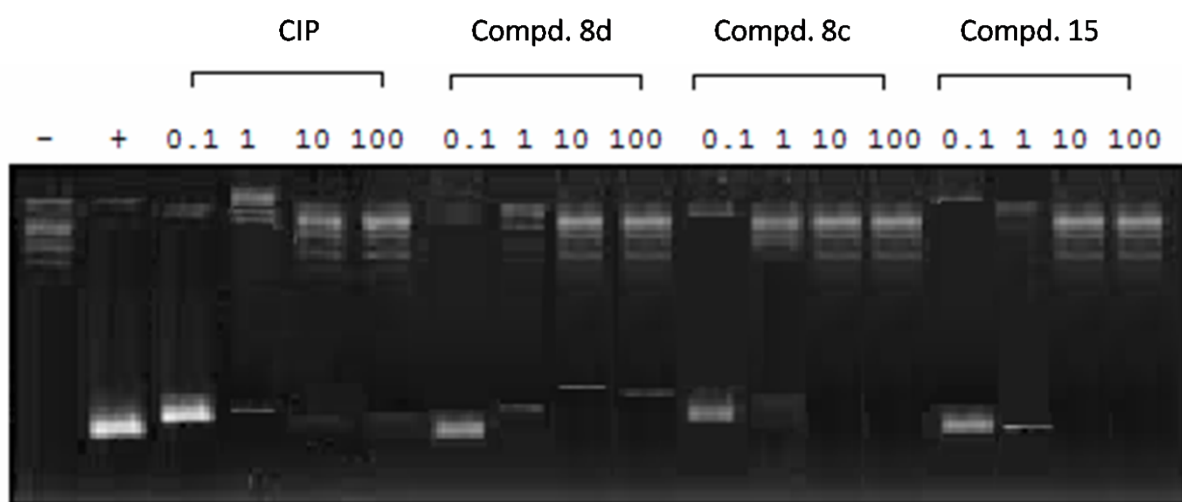
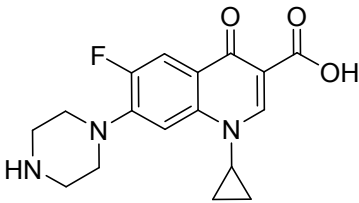
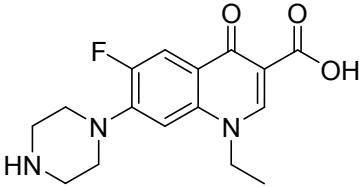
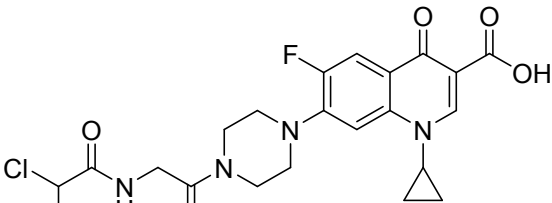
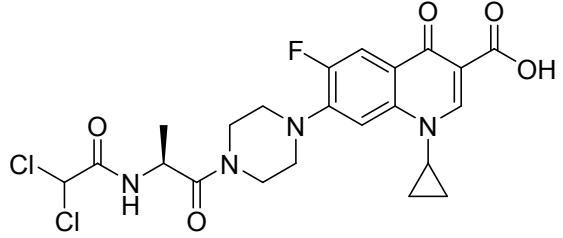
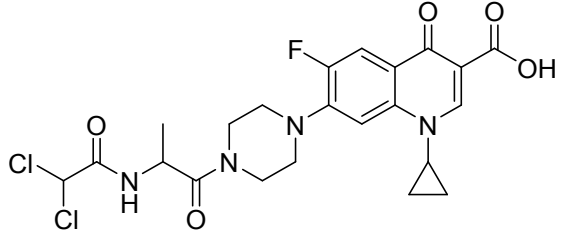
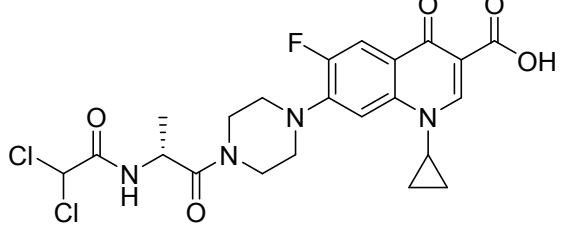
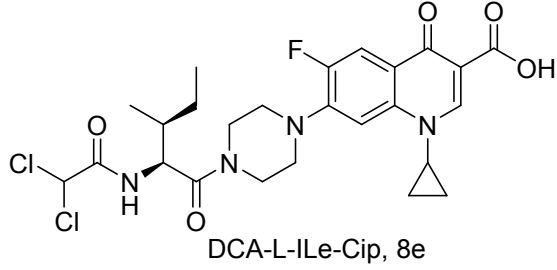
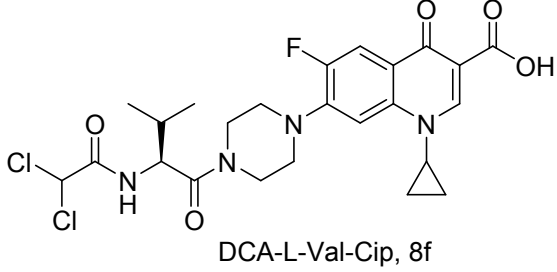
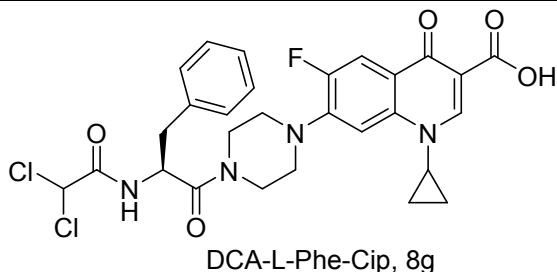


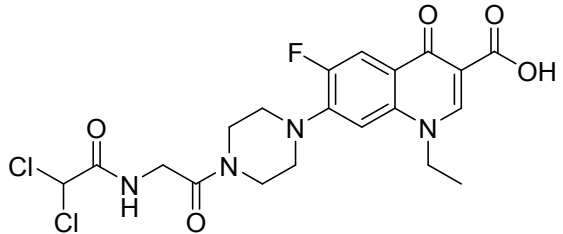
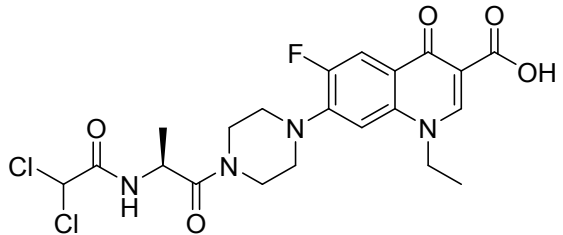
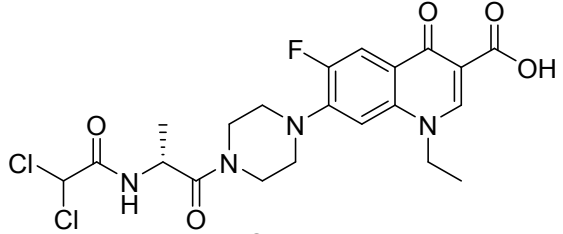
Fig. 2. Preview depicting the *E. coli* DNA gyrase supercoiling assay of CIP, conjugates **8c**, **8d** and **15** at different concentrations (0.1, 1, 10, and 100 μM).

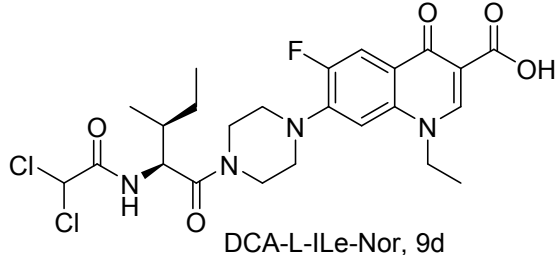
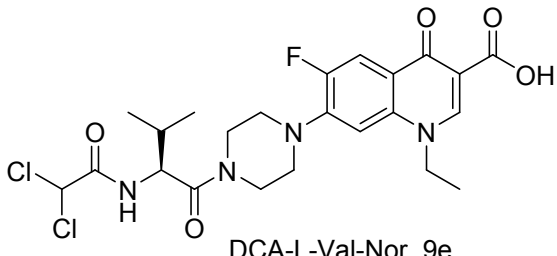
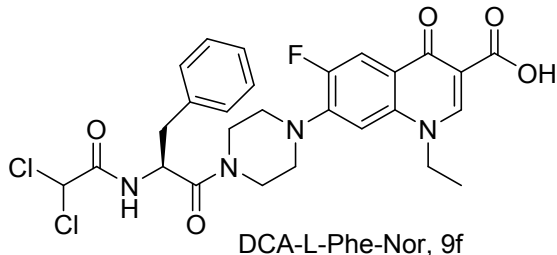
Table 1. Antimicrobial properties of the tested compounds (**8a–g**, **9a–f**, **15**, **16**) and standard references (**6**, **7**).

Entry	Compd.	Minimum inhibitory concentration (MIC), $\mu\text{g/mL}$ (μM)			
		<i>E. coli</i>	<i>P. aeruginosa</i>	<i>S. aureus</i>	<i>E. faecalis</i>
1	 <p>CIP, 6</p>	0.125 (0.377)	1.667 (5.030)	4.000 (12.072)	8.000 (24.144)
2	 <p>NOR, 7</p>	2.000 (6.263)	4.000 (12.526)	26.667 (83.506)	32.000 (100.207)
3	 <p>DCA-Gly-Cip, 8a</p>	0.333 (0.668)	9.333 (18.692)	0.750 (1.502)	2.000 (4.005)

4	 <p>DCA-L-Ala-Cip, 8b</p>	0.667 (1.299)	21.333 (41.557)	0.250 (0.487)	1.667 (3.247)
5	 <p>DCA-DL-Ala-Cip, 8c</p>	0.100 (0.195)	5.333 (10.389)	0.100 (0.195)	0.600 (1.169)
6	 <p>DCA-D-Ala-Cip, 8d</p>	0.082 (0.159)	4.000 (7.792)	0.167 (0.325)	1.500 (2.922)

7	 <p>DCA-L-Ile-Cip, 8e</p>	0.333 (0.600)	10.667 (19.204)	0.267 (0.480)	3.733 (6.722)
8	 <p>DCA-L-Val-Cip, 8f</p>	0.333 (0.616)	17.067 (31.523)	0.333 (0.616)	0.800 (1.478)
9	 <p>DCA-L-Phe-Cip, 8g</p>	0.800 (1.357)	25.600 (43.430)	1.067 (1.810)	4.267 (7.238)

10	 <p>DCA-Gly-Nor, 9a</p>	1.667 (3.420)	64.000 (131.333)	16.000 (32.833)	53.333 (109.444)
11	 <p>DCA-L-Ala-Nor, 9b</p>	4.667 (9.308)	128.000 (255.316)	6.667 (13.298)	21.333 (42.553)
12	 <p>DCA-D-Ala-Nor, 9c</p>	1.000 (1.995)	13.333 (26.595)	1.000 (1.995)	6.867 (13.697)

13	 <p>DCA-L-Ile-Nor, 9d</p>	6.400 (11.777)	>51.3 (>94.402)	2.133 (3.926)	25.600 (47.109)
14	 <p>DCA-L-Val-Nor, 9e</p>	5.333 (10.074)	>51.3 (>96.904)	2.133 (4.030)	21.350 (40.329)
15	 <p>DCA-L-Phe-Nor, 9f</p>	5.333 (9.236)	>51.3 (>88.842)	2.667 (4.618)	>51.3 (>88.842)

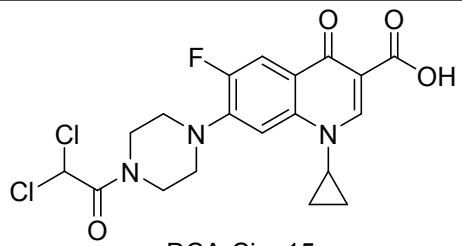
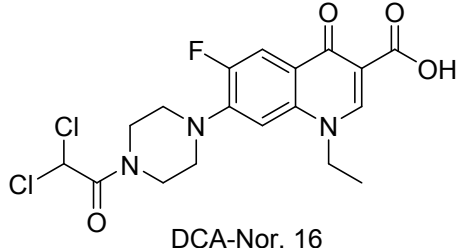
16	 <p>DCA-Cip, 15</p>	0.030 (0.068)	2.000 (4.522)	0.125 (0.283)	1.167 (2.638)
17	 <p>DCA-Nor, 16</p>	0.250 (0.581)	9.333 (21.692)	1.000 (2.324)	5.333 (12.396)

Table 2. Inhibitory properties of *E. coli* DNA gyrase supercoiling for the tested compounds.

Entry	Compd.	IC ₅₀ (μM) ± SD
1	6 (CIP)	2.27 ± 0.16
2	8c	3.25 ± 0.11
3	8d	9.80 ± 0.42
4	15	3.55 ± 0.17